JOURNAL OF AGRICULTURAL AND FOOD CHEMISTRY

Effect of Stirring and Seeding on Whey Protein Fibril Formation

SUZANNE G. BOLDER,[†,‡] LEONARD M. C. SAGIS,[‡] PAUL VENEMA,[‡] AND ERIK VAN DER LINDEN*[,‡]

DMV International b.v., P.O. Box 13, 5460 BA Veghel, The Netherlands, Food Physics Group, Department of Agrotechnology and Food Sciences, Wageningen University, P.O. Box 8129, 6700 EV Wageningen, The Netherlands

The effect of stirring and seeding on the formation of fibrils in whey protein isolate (WPI) solutions was studied. More fibrils of a similar length are formed when WPI is stirred during heating at pH 2 and 80 °C compared to samples that were heated at rest. Addition of seeds did not show an additional effect compared to samples that were stirred. We propose a model for fibril formation, including an activation, nucleation, growth, and termination step. The activation and nucleation steps are the rate-determining steps. Fibril growth is relatively fast but terminates after prolonged heating. Two processes that possibly induce termination of fibril growth are hydrolysis of nonassembled monomers and inactivation of the growth ends of the fibrils. Stirring may break up immature fibrils, thus producing more active fibrils. Stirring also seems to accelerate the kinetics of fibril formation, resulting in an increase of the number of fibrils formed.

KEYWORDS: Heat-induced aggregation; fibrils; whey proteins; stirring; seeding

INTRODUCTION

Many proteins are known to form fibrils under mildly denaturing conditions (*1*, *2*). Various types of food proteins, like whey proteins (*3*−*12*), soy proteins (*13*), and egg-white proteins (*14*−*19*), also form fibrils under specific conditions. Whey proteins are commonly used as food ingredients in a wide range of applications such as desserts, beverages, confectionary, dairy products, and meat products for their emulsifying, stabilizing, foaming, or gelation properties. Commercial whey protein ingredients, for example, whey protein isolates (WPIs), are composed of mixtures of proteins. The most abundant whey protein is β-lactoglobulin (β-lg). Other globular whey proteins are α-lactalbumin (α-lac) and bovine serum albumin (BSA). Whey proteins, and specifically β-lg, are known to form fibrils upon heating at pH 2 and low ionic strength (*3*, *6*, *8*−*11*, *20*−*26*). Their ability to form fibrils is interesting because of the potential use as functional ingredients in food products. The common treatment for making whey protein fibrils is by prolonged heating of aqueous whey protein solutions at pH 2 and low ionic strength at temperatures exceeding the denaturation temperature of the protein. To optimize the fibril formation, we are interested in the assembly kinetics of whey proteins into fibrils. In a previous paper, we studied the heat-induced conversion of whey protein monomers into fibrils during heating at rest at 80 °C (*27*). The conversion was found to vary from about 5% for 0.5 wt % WPI solutions to about 45% for 5 wt % WPI solutions.

In this paper, we examine the effects of stirring and seeding on the conversion of whey proteins into fibrils. For scale-up of the process of whey protein fibril formation, it would be desirable to accelerate the process by decreasing the heating time or increasing the conversion, thus improving the process efficiency. From the literature, it is known that the addition of preformed fibrils (seeding) and the application of shear can enhance fibril formation. Krebs et al. (*15*) showed that seeding accelerates the fibril formation of hen lysozyme. Nielsen et al. (*28*) reported that both seeding and vigorous agitation enhance insulin fibril formation. Sonication was found to induce fibril formation in diverse proteins (*29*). Hill et al. (*30*) and Akkermans et al. (*3*) both showed that shear flow enhances fibril formation in heat-denatured β-lg samples. Here we study the effects of both stirring and seeding on WPI fibril formation. We have determined the conversion as a function of heating time using a method that we developed based on centrifugal filtration (*27*). We also used flow birefringence measurements to determine the length distribution of the fibrils and measured the apparent viscosity of the samples.

EXPERIMENTAL PROCEDURES

Sample Preparation. BiPRO whey protein isolate (WPI) was obtained from Davisco Foods International, Inc. (Le Sueur, MN). All the other chemicals used were of analytical grade. WPI samples were prepared and purified as described previously (see refs 20 and 27). The purified WPI contains about 65% β-lg (*20*, *27*, *31*). The stock solution was diluted to 2 wt % WPI with HCl solution of pH 2. Samples of 20 mL WPI solution were heated in sealed glass vessels in a metal heating plate in combination with a magnetic stirrer, at 80 °C (±2 °C). In Table 1, an overview is given of the treatment of the various sample series studied.

* Corresponding author. E-mail address: erik.vanderlinden@wur.nl. Telephone: +31 317 485417. Fax: +31 317 483669.
† DMV International b.v.
‡ Wageningen University.

10.1021/jf063351r CCC: $37.00
Published on Web 06/16/2007

Table 1. Overview of Sample Treatment of the Various Sample Series Studied

series	WPI concentration [wt %]	treatment	seeds[a] [wt %]
R0	2	rest	0
S0	2	stirred	0
S10	2	stirred	10
S30	2	stirred	30

[a] Seeds were prepared by heating a 2 wt % WPI solution for 10 h at pH 2 at 80 °C while stirring constantly. The seeds concentration is [wt %] of the total WPI concentration.

To study the effect of stirring on the fibril formation, samples were heated at rest (series R0) or while being stirred constantly (at a rate of about 200 rpm) with a magnetic stirring bar (series S0). Besides the effect of stirring, we have also examined the effect of seeding on the whey protein fibril formation. Seeding is the addition of preformed fibrils to WPI samples prior to the heat treatment. Seeds were prepared by heating a 2 wt % WPI solution for 10 h at pH 2 and 80 °C while stirring constantly. After heating, the sample was cooled on ice water and kept at 0 °C overnight. Seeds solutions and unheated whey protein solutions were mixed in various ratios. Both samples (WPI seeds and unheated WPI) had the same overall WPI concentration of 2 wt %. Therefore the total WPI concentration was constant, independent of the concentration of seeds added. The concentrations of seeds added were: 0% seeds (series S0), 10% seeds (S10), or 30% seeds (S30). The seeded samples were heated at pH 2 and 80 °C while being stirred constantly.

After various heating times between 0 and 24 h, samples were taken out of the heating plate and immediately cooled on ice water.

Conversion Experiments. To determine the degree of conversion of whey protein monomers into aggregates, the centrifugal filtration method as described in Bolder et al. (*27*) was used. An unheated whey protein sample was included as a control in every experiment, and the total protein recovery (filtrate + retentate) was in a range of 95−100%. The experiments were repeated three times for all R0 samples and for the stirred samples that were heated for 10 h. The average values were plotted with the error bars indicating the maximum deviation from the mean.

Rheo-optical Measurements. *Theory.* Rheo-optics is a method used to study the relationship between flow properties and structure of materials (*32*). Rogers et al. (*10*) developed a method to determine the concentration and length distribution of β-lactoglobulin fibrils quantitatively from the decay curves of birefringence measurements. Samples were subjected to steady shear flow of 5 s^{-1}. After cessation of the shear, the decay of flow-induced birefringence was measured. This decay is analyzed using the Doi−Edwards−Marrucci−Grizzuti theory (DEMG) (*34*−*36*), assuming that β-lg fibrils are free, unbranched, nonsticky rods and samples are in the semidilute regime (*10*). According to the method by Rogers et al. (*10*), the flow-induced birefringence, $\Delta n'$, is proportional to the total length of the fibrils as

$$\Delta n' = M \int c \cdot L \cdot \mathrm{d}L \tag{1}$$

where M is a constant equal to the birefringence per unit length of the fibrils, as determined by Rogers et al. (*10*) for pure β-lactoglobulin fibrils, and c is the concentration of fibrils with a length between L and $L + \mathrm{d}L$.

Testing whether the samples are semidilute can be done by analyzing the scaling of the decay of birefringence with concentration. If samples are in the semidilute regime, the birefringence in steady shear flow is concentration-dependent and scales according to ref *10*

$$\nu \Delta n' = f(\dot{\gamma}/\nu^2, \nu^2 t) \tag{2}$$

where ν is the dilution factor and $\dot{\gamma}$ is the shear rate. If fibrils are short enough or dilute enough so that they do not interact with each other, the diffusion of the fibrils is independent of the concentration. The flow-induced birefringence then scales according to (*10*):

$$\nu \Delta n' = f(\dot{\gamma}, t) \tag{3}$$

Equipment. Rheo-optical measurements on the WPI fibrils, prepared as described above, were performed using a strain-controlled ARES rheometer (Rheometrics Scientific) equipped with a modified optical analysis module (*33*). Measurements were performed in a Couette geometry with a static inner bob of diameter 30 mm and rotating outer cup (with a quartz bottom plate) of diameter 33.8 mm. A laser beam of wavelength 670 nm (5 mW) passed vertically between the cup and bob through the sample. In this setup, the apparatus was capable of measuring birefringence, $\Delta n'$, to values as low as 10^{-8} at a sampling frequency of 24 Hz. The optical signal from the detector was digitized using an analogue-to-digital converter and analyzed using Labview (National Instruments). The rheo-optical experiments were performed in an air-conditioned room at 20 °C (±1 °C).

Measuring Flow-Induced Birefringence and Fibril Length Distribution. WPI fibril solutions were subjected to a shear rate sweep with shear rates ranging from 0.1 to 200 s^{-1}. All shear rates were applied for 30 s. At each shear rate, the flow-induced birefringence was measured. During the 30 s of applying the shear, the birefringence was constant, indicating that the steady shear flow did not damage the fibrils. This was also reported by Rogers et al. and Akkermans et al. for pure β-lg fibrils (*3*, *10*).

The samples were also subjected to steady shear flow at a shear rate of 5 s^{-1} during 60 s to determine the length distribution. After cessation of the flow, the decay curve of the birefringence was measured. This was measured both for clockwise and counterclockwise rotation during the shear step. The decay-time strongly depends on the length and the concentration of the fibrils. Several dilutions were made for most samples to make sure to be in the semidilute regime (no permanent birefringence) and in order to reduce the decay time to a reasonable measuring time. From the decay curves measured, the fibril length distribution was calculated using the method developed by Rogers et al. (*10*).

Viscosity Measurements. Shear rate sweeps were performed for the various whey protein samples and their dilutions. A PAAR Physica MCR301 stress-controlled rheometer with a concentric cylindrical double gap geometry (DG 26.7) was used to perform the rheological measurements. The dependence of the apparent viscosity of the samples was measured as a function of the shear rate (temperature 20 °C, shear rate range 0.001−1000 s^{-1}). The shear rate was increased logarithmically. Measurements were repeated three times. No change in the apparent viscosity was measured for subsequent measurements, again indicating that the experiment did not affect the sample.

RESULTS

Effect of Stirring on Appearance of the Samples. The appearance of 2 wt % WPI samples was studied for samples heated at rest and for samples that were continuously stirred during heating. Stirred samples were all stirred at the same rate of about 200 rpm. An example of both a sample heated at rest and a sample that was stirred during heating, observed at rest between crossed polarizers, is shown in **Figure 1**. These samples were heated for 10 h at 80 °C and subsequently cooled. The appearance of the samples did not change as a result of the cooling step. Heating the samples at rest resulted in samples containing many spherulites, as was also described in our earlier study and in literature (*6*, *20*, *25*). Upon gentle shaking, the continuous phase surrounding the spherulites shows flow-induced birefringence, caused by flow-induced alignment of the fibrils that coexist with the spherulites (*20*). Samples that were stirred during heating did not contain spherulites. Instead, strong permanent birefringence was observed when studying these samples at rest between crossed polarizers. The stirred samples appeared more viscous than the samples heated at rest. Viscosity measurements confirmed this observation (see section on apparent viscosity below).

Figure 1. Picture of samples observed at rest between crossed polarizers. The samples were heated for 10 h at 80 °C, pH 2, and 2 wt % WPI. The left sample was heated at rest, and the right sample was heated while being stirred constantly.

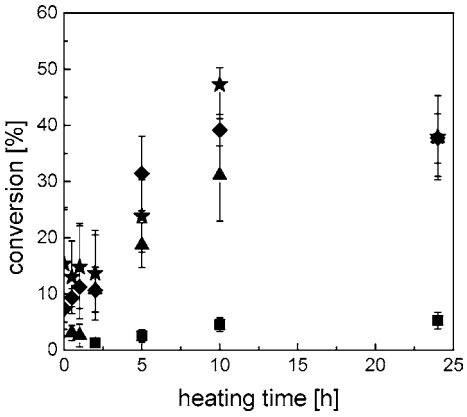

Figure 2. Conversion determined with the centrifugal filtration method as a function of the heating time for various sample series: R0 (■), S0 (▲), S10 (◆), S30 (★). Samples were heated at 2 wt % WPI at pH 2 and 80 °C. Error bars indicate the maximum deviation from the mean values.

Effect of Stirring and Seeding on the Conversion. The conversion, which we define as the percentage of aggregated protein material in the sample, was determined as a function of the heating time. Four sample series were studied in order to study the effect of both stirring and addition of seeds on the conversion, as indicated in Table 1. The results presented in **Figure 2** show that the conversion for samples that were stirred during heating (S0) is significantly higher than for samples heated at rest (R0). The conversion of protein monomers into aggregates increases with heating time. This was also observed in previous work (*5*, *26*, *27*, *37*). When comparing the conversion between sample series that were heated in the presence of various seeds concentrations (S0, S10, and S30), no significant differences were observed after long periods of heating. Only at short heating times were differences observed. These differences in conversion were caused by the preformed fibrils that were added to the samples prior to heating. Therefore, in our experiments, seeding did not affect the conversion of WPI monomers into fibrils when samples were stirred during heating. Seeding might have an effect on the fibril growth in the early stages of fibril formation, but this is not observed in our results. The largest effect on the conversion that we observed in our experiments is the effect of stirring during heating. This drastically increased the conversion (by about a factor of 8) compared to nonstirred samples.

Effect of Stirring and Seeding on Flow-Induced Birefringence and Length Distributions. *Steady Shear Birefringence and Concentration Scaling.* In **Figure 3A**, the steady shear birefringence, corrected for the dilution factor of the samples, $\nu\Delta n'$, is plotted as a function of the heating time. **Figure 3B** shows the steady shear birefringence, $\Delta n'$, plotted as a function of the shear rate for the various sample series studied. The birefringence shows a significant difference between the samples heated at rest (R0) and the samples that were stirred during heating (S0). The samples that were heated at rest were difficult to measure because of weak birefringence. The presence of spherulites in the samples also disturbed the birefringence signal. Only after heating the R0 samples for 5 h was a detectable birefringence induced. The birefringence signal further increased with heating time. The samples that were stirred during heating (S0) and in the presence of various seeds concentrations (S10 and S30) show a much higher birefringence signal than the samples that were heated at rest. This is confirmed by the visual observations of the samples with polarized light (**Figure 1**). Strong permanent birefringence was observed in samples that were stirred during heating compared to the weak flow-induced birefringence detected in samples that were heated at rest (see **Figure 1**). Samples in the presence of seeds (S10 and S30) show similar birefringence compared to the samples without seeds (S0) (**Figure 3**). This is consistent with the results for the conversion as a function of heating time (**Figure 2**).

At the start of the shear rate sweep, the birefringence was low for all samples (**Figure 3B**). The R0 sample showed only weak flow-induced birefringence. The samples that were stirred during heating (S0, S10, and S30) showed a sharp increase in birefringence with increasing shear rate. The birefringence appears to reach a plateau for high shear rates, where fibrils are totally aligned (**Figure 3B**).

In **Figure 4A**, the birefringence under steady shear is shown for a WPI fibril solution at various dilutions. These results are representative for all samples studied. In **Figure 4B**, the steady shear birefringence, corrected for the dilution factor, $\nu\Delta n'$, is plotted according to the dilute regime (eq 2) and in **Figure 4C** according to the semidilute regime (eq 3). At low shear rates, the curves meet when scaled according to the semidilute regime, while at high shear rates, the curves meet when scaled according to the dilute regime or concentration-independent regime. This shows that the system changes from semidilute to dilute behavior with increasing shear rates.

Decay Curves and Length Distributions. **Figure 5** shows the decay curves in stopped flow for successive dilutions of a WPI fibril solution. For all samples, a shear rate was chosen of 5 s^{-1} to ensure that the system is still in the semidilute regime and not in the dilute regime ($\dot{\gamma} > 30\ s^{-1}$, see **Figure 4B,C**). At a shear rate of 5 s^{-1}, the system is slightly outside the semidilute regime, but still far removed from the dilute regime (see **Figure 4B,C**). Choosing a lower shear rate would induce insufficient alignment to measure the decay accurately (for details, see Rogers et al. (*10*)). The decay of the birefringence becomes faster upon further dilution of the samples. The initial birefringence also decreases because of the lower fibril concentration in the samples upon successive dilutions. The decay curves were used to calculate the length distributions. In **Figure 6**, an example of length distributions for various heating times is shown for the S10 samples that were diluted four times. Similar results were observed for all sample series and all dilution factors measured. From the length distribution curves for various heating times (**Figure 6**), it is clear that the peak fibril length, L_{peak}, remains almost constant for increasing heating times (also see **Figure 7**). Only a slight decrease of L_{peak} can be observed with increasing heating time. The height of the length distribution curve clearly increases with increasing heating time,

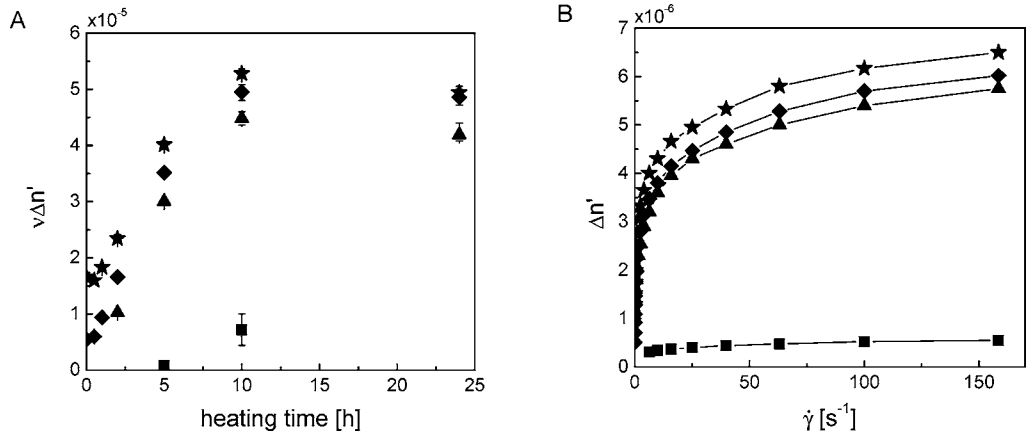

Figure 3. **(A)** Steady shear birefringence corrected for the dilution factor of the sample, $\nu\Delta n'$, as a function of the heating time. Error bars indicate the variation between the clockwise and counterclockwise measurements. Samples were all heated at 2 wt % WPI at pH 2 at 80 °C. **(B)** Steady shear birefringence, $\Delta n'$, as a function of the shear rate, $\dot{\gamma}$, for samples that were heated for 10 h at 2 wt % WPI at pH 2 at 80 °C. Samples were measured at $\nu = 8$. Data points are connected with straight lines for visualization. Symbols represent various sample series: R0 (■), S0 (▲), S10 (♦), S30 (★).

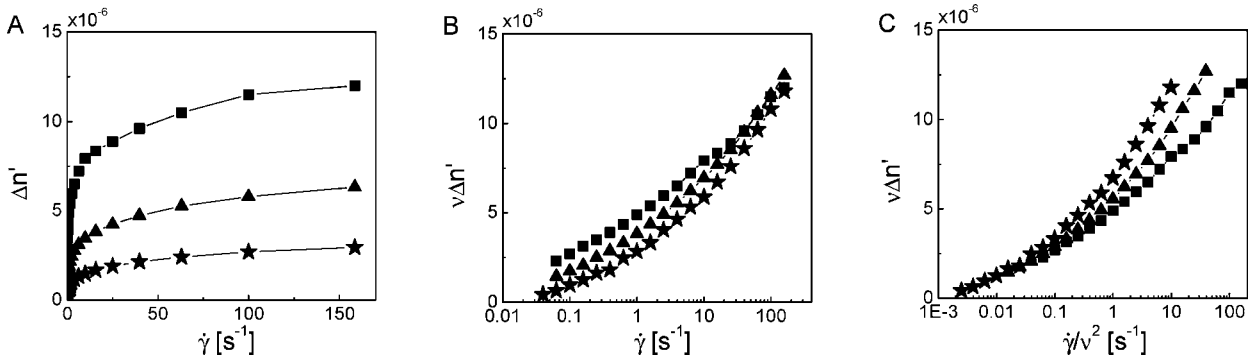

Figure 4. **(A)** Steady shear birefringence, $\Delta n'$, as a function of the shear rate, $\dot{\gamma}$, for different dilutions, ν, of WPI fibril solutions (that were stirred during heating for 24 h in the presence of 10% seeds, S10); scaled according to the dilute **(B)** and semidilute **(C)** regimes. $\nu = 4$ (■), $\nu = 8$ (▲), $\nu = 16$ (★).

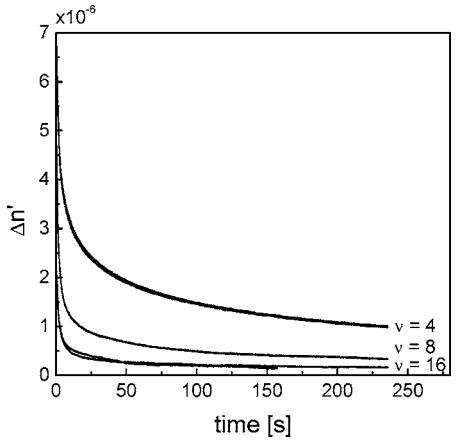

Figure 5. Birefringence decay curves measured for various dilutions of WPI fibril solutions (that were stirred during heating for 10 h in the absence of seeds, S0). Decay curves are measured after cessation of the flow induced by a shear rate $\dot{\gamma} = 5\ s^{-1}$ for clockwise and counter clockwise rotation during shear flow.

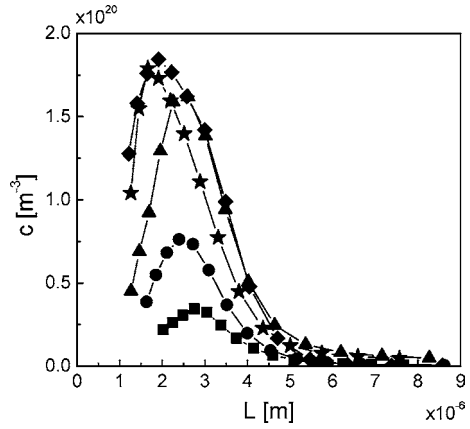

Figure 6. Length distributions of WPI fibrils that were prepared while stirring during heating in the presence of 10% seeds (S10) upon various heating times at 2 wt % WPI at pH 2 and 80 °C: 1 h (■), 2 h (●), 5 h (▲), 10 h (◆), 24 h (★). The samples were all diluted 4 times prior to measuring the decay curves after cessation of the flow induced by a shear rate of 5 s^{-1}.

followed by a slight decrease for heating times exceeding 10 h. In parts **A** and **B** of **Figure 7**, we have plotted the peak fibril length, L_{peak} (**A**), and the peak concentration, corrected for the dilution, νC_{peak} (**B**), as a function of the heating time for the various sample series studied. From **Figure 7A** it is clear that L_{peak} does not change significantly with heating time or with the concentration of seeds added. Only for samples heated at rest (R0) is L_{peak} slightly higher than for the samples that were heated under shear. **Figure 7B** shows that νC_{peak} increases with heating time, showing a significant difference between samples that were heated at rest (R0) and samples that were stirred during heating. Only for short heating times was a difference observed for samples that were heated in the presence of seeds. This is due to the added preformed fibrils. All sample series show a slight decrease in length distributions for heating times exceeding 10 h. This suggests decomposition of part of the fibrils after very long heating times. This is in line with results presented for the conversion as a function of heating time (see **Figure 2**),

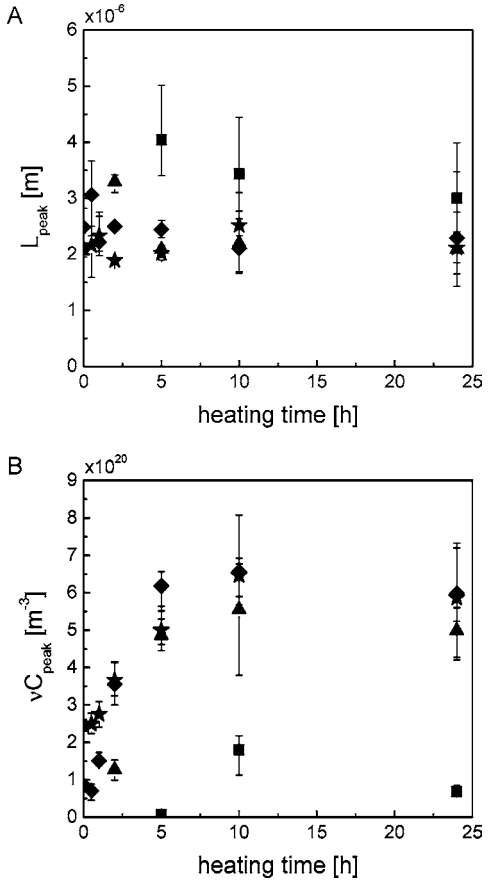

Figure 7. **(A)** The peak fibril length, L_{peak}, and **(B)** the peak length distribution corrected for the dilution factor, νC_{peak}, for the length distributions as a function of the heating time for various sample series: R0 (■), S0 (▲), S10 (◆), S30 (★). Samples were heated at 2 wt % WPI at pH 2 at 80 °C. The values were averaged over the measurements of all decay curves after cessation of the flow induced by a shear rate, $\dot{\gamma}$ of 5 s^{-1}.

where a slight decrease in conversion is observed for heating times exceeding 10 h. The shape of the curves in **Figure 7B** is consistent with the curves in **Figure 2**. The results of the birefringence measurements can be used to determine the conversion, as described in a following paper (*38*).

Effect of Stirring and Seeding on Apparent Viscosity. The apparent viscosity was measured as a function of shear rate. The curves measured for various heating times of one sample series (S0) are plotted in **Figure 8**. For short heating times, the apparent viscosity does not change. The viscosity of the unheated WPI solution is slightly higher than that of the pH 2 solution (the solvent). The heated protein samples have an increased apparent viscosity and are shear thinning. The apparent viscosity increases with heating time. For heating times exceeding 10 h, a slight decrease in viscosity is measured. In **Figure 9**, the apparent viscosity measured as a function of the shear rate is plotted for undiluted samples that were heated for 10 h under various conditions. The samples that were stirred during heating show a much higher viscosity than the samples that were heated at rest. The samples in the presence of various seeds concentrations have the same viscosity, independent of the seeds concentration (0%, 10%, or 30% seeds). The curves for S0, S10, and S30 were fitted, giving a slope of −0.71. This is close to a value of −0.5, which is the theoretical value typical for polydomain liquid crystalline behavior (*39*). For polydomain liquid crystalline systems, one would expect first an increase, followed by a decrease in viscosity upon increasing dilutions

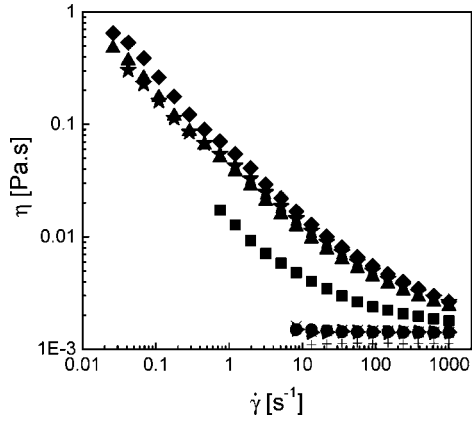

Figure 8. Apparent viscosity as a function of shear rate after various heating times. Samples were heated for various heating times at 2 wt % WPI at pH 2 and 80 °C, while being stirred, in the absence of seeds (S0 samples). pH 2 solution (the solvent) (+), 0 h (×), 0.5 h (right-pointing solid triangle), 1 h (●), 2 h (■), 5 h (▲), 10 h (◆), 24 h (★).

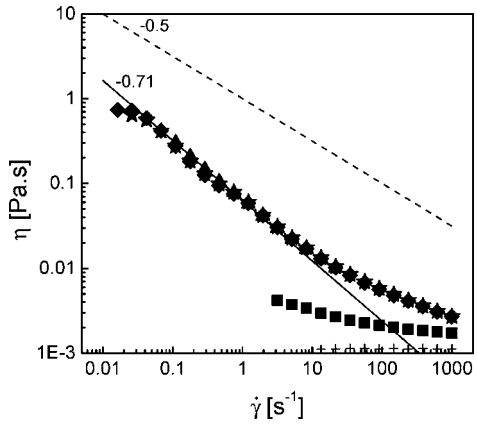

Figure 9. Apparent viscosity as a function of shear rate for various sample series: pH 2 solution (+), R0 (■), S0 (▲), S10 (◆), S30 (★). Samples were heated for 10 h at 2 wt % WPI at pH 2 at 80 °C. These are the undiluted heated samples. The dotted line is a line with a slope of –0.5. The solid line is the line fitted to the curves for S0, S10, and S30, where the slope is constant. The slope of this line is –0.71.

(*40*). As shown in **Figure 1**, the samples that were stirred during heating show domains with permanent birefringence. Upon diluting our samples, a decrease in the apparent viscosity was observed upon successive dilution (results not shown). No maximum for the viscosity was observed upon diluting our samples. This suggests that our undiluted heated samples are not in the polydomain liquid crystalline regime but that they are in the biphasic regime with nematic regions in an isotropic phase.

DISCUSSION

The experiments described here show an increase in the conversion, the birefringence, and the apparent viscosity measured for WPI samples that were being stirred constantly during heating compared to samples that were heated at rest. Under the conditions used (pH 2 and low ionic strength), fibrils form upon heating WPI solutions (*9*, *20*, *27*, *31*). Our previous work indicates that, under the conditions used, β-lactoglobulin is the only whey protein involved in fibril formation (*20*, *27*, *31*). At pH 2, WPI proteins have a net positive charge, resulting in high electrostatic repulsion between the monomers (*5*, *41*). WPI proteins are (at least partially) denatured during heating

above their denaturation temperature. Denaturation leads to unfolding of the globular protein structure and the exposure of groups that are buried in the core of the globular protein in the native state. The partial unfolding and possible additional change in the protein structure (e.g., deamidation (*42*)) may serve as an activation step for protein aggregation.

In earlier work we found that, in WPI samples that are heated at rest, fibrils and spherulites coexist, indicating that fibrils and spherulites form simultaneously (*20*). This coexistence of fibrils and spherulites was also observed for silkmoth chorion and for pure β-lactoglobulin (*6*, *43*). Spherulites are composed of fibrils that grow radially outward from a nucleus (*6*, *20*, *44*−*46*). This nucleus may be composed of small (random) protein aggregates or oligomers (*1*, *44*−*46*), axialites (*6*, *47*), or droplets formed by liquid−liquid phase separation (*48*−*50*). Fibrils nucleate both free in solution and on spherulite nucleation sites (*20*, *44*). Spherulites are formed only in a certain concentration range for WPI samples (*20*). At WPI concentrations above 6 wt %, spherulites are no longer observed. Instead, liquid crystalline phases are formed upon heating WPI at pH 2 (*20*). The conversion of WPI monomers into fibrils increases with concentration (*27*) and when samples are stirred. When more monomers are converted into fibrils, the transition to a poly domain liquid crystalline phase will occur at a lower total WPI concentration (*20*, *25*). Spherulite formation is very slow compared to fibril growth (spherulites are observed only after 2 h of heating a 2 wt % WPI solution) (*20*), while the transition to a liquid crystalline or gel-like phase is rapid at high fibril concentrations. At high protein concentrations, and therefore high amounts of fibrils, the transition to a liquid crystalline phase can occur before spherulites have formed, thus inhibiting formation of spherulites (*16*, *20*).

In our current experiments, we observed that no spherulites form when WPI samples are stirred continuously during heating. The exact mechanism behind this is unclear. Stirring induces a complex flow profile, including elongational flow and vortices, but disruption of nuclei is unlikely because they are too small to be affected by flow. A possible explanation for the absence of spherulites in stirred samples could be that due to stirring the reaction kinetics for fibril formation accelerate and that therefore no spherulites can be formed.

The increase in conversion, birefringence, and apparent viscosity measured for samples that were stirred during heating compared to samples that were heated at rest, combined with the absence of spherulites, indicates that more fibrils are formed in stirred samples. Two possible explanations for these findings are that flow may disrupt growing, immature fibrils, producing a higher number of active fibrils for fibril formation or that the application of flow during heating increases both the number of growing fibrils and the encounters between activated protein monomers and between monomers and the growing fibrils. The chance of binding will therefore be higher and, as a result, more protein material will be incorporated into fibrils (resulting in either more or longer fibrils). This is in agreement with results reported by Hill et al. (*30*) and Akkermans et al. (*3*). They show for pure β-lactoglobulin an increase in Thioflavin T fluorescence and birefringence for samples heated under shear compared to samples heated at rest.

The length distribution results show that the length, L_{peak}, of the fibrils formed upon heating WPI, does not significantly change for various treatments of the samples nor with heating time (**Figure 7A**). The peak concentration, C_{peak}, does increase with heating time, reaching a maximum at around 10 h (**Figure 7B**). For heating times exceeding 10 h, a decrease is observed in the conversion (**Figure 2**), the birefringence (**Figure 3A**), the peak concentration (**Figure 7B**), and the apparent viscosity measured (**Figure 8**), suggesting a possible breakdown of fibrils upon extended heating times.

Conversion, birefringence, and apparent viscosity results suggest that the addition of seeds (containing nonassembled monomers and fibrils) did not result in an additional increase in the conversion. The seeds that we used had been heated for 10 h. When adding these preformed fibrils to a fresh solution, the fibrils may have already undergone some type of termination step and are therefore no longer susceptible to additional growth. The nonassembled monomers have likely been hydrolyzed and therefore become unable to assemble (*27*). The kinetics of WPI fibril formation is not affected by the addition of seeds. The curves for samples heated without added seeds (S0) and for samples heated in the presence of seeds (S10 and S30) are almost identical (see **Figures 2**, **3A**, and **7B**). If seeding would affect the kinetics significantly, the curves for S10 and S30 would have started steeper than the curve for S0.

The seeds concentration does not affect the apparent viscosity obtained after long heating times (**Figure 9**), indicating that a similar amount of fibril material is present after prolonged heating. For short heating times, the samples in the presence of seeds show a slightly higher apparent viscosity than samples without added seeds (results not shown). This is caused by the presence of preformed fibrils.

In our previous work, we have shown that fibrils are formed upon heating WPI solutions at pH 2 and that no native proteins remain (*27*). The nonassembled protein is mildly hydrolyzed upon prolonged heating. This might result in inactivation of the monomers for assembly, leading to termination of fibril formation due to lack of active protein material after prolonged heating. Rogers et al. (*51*) suggest that pure β-lg fibrils are composed of monomers that are joining head-to-tail. If the monomers change due to for example hydrolysis, they may no longer be susceptible to assembly. A definite proof of this hypothesis could only be given by disassembling the fibrils into their building blocks without damaging the structure of these building blocks or chemically degrading them. The fibrils are however very stable, and a suitable method to disassemble them is not yet available.

These results indicate that WPI fibril formation is a nucleation and growth process. The growth of the fibrils is relatively fast, and the activation and nucleation steps appear to be the rate-determining steps. During the assembly of WPI monomers into fibrils, monomers first bind reversibly, followed by a change that irreversibly binds them. This change is likely to be a conformational change, which involves formation of intermolecular β-sheets (*6*, *23*, *51*, *52*). Recent studies of β-lg fibrils have shown that their X-ray fiber diffraction pattern is indicative of the cross-β motif, that they bind the cross-β sheet specific dyes Thioflavin T and Congo red, and that they show increased β-sheet content relative to their native state (*6*, *23*, *51*, *52*).

Fibril formation terminates when no reactive monomers are present due to hydrolysis, or when all fibril ends are inactivated, possibly due to formation of intermolecular β-sheets or due to hydrolysis of fibril ends.

On the basis of our results, we propose the following (schematic) model for fibril formation at rest (lower part) or while stirred during heating (upper part) (**Figure 10**). The first step is the activation of the native monomers by heat denaturation at low pH, inducing partial unfolding of the proteins. The active monomers are able to assemble and form nuclei. This includes both nuclei for spherulites and for fibril formation.

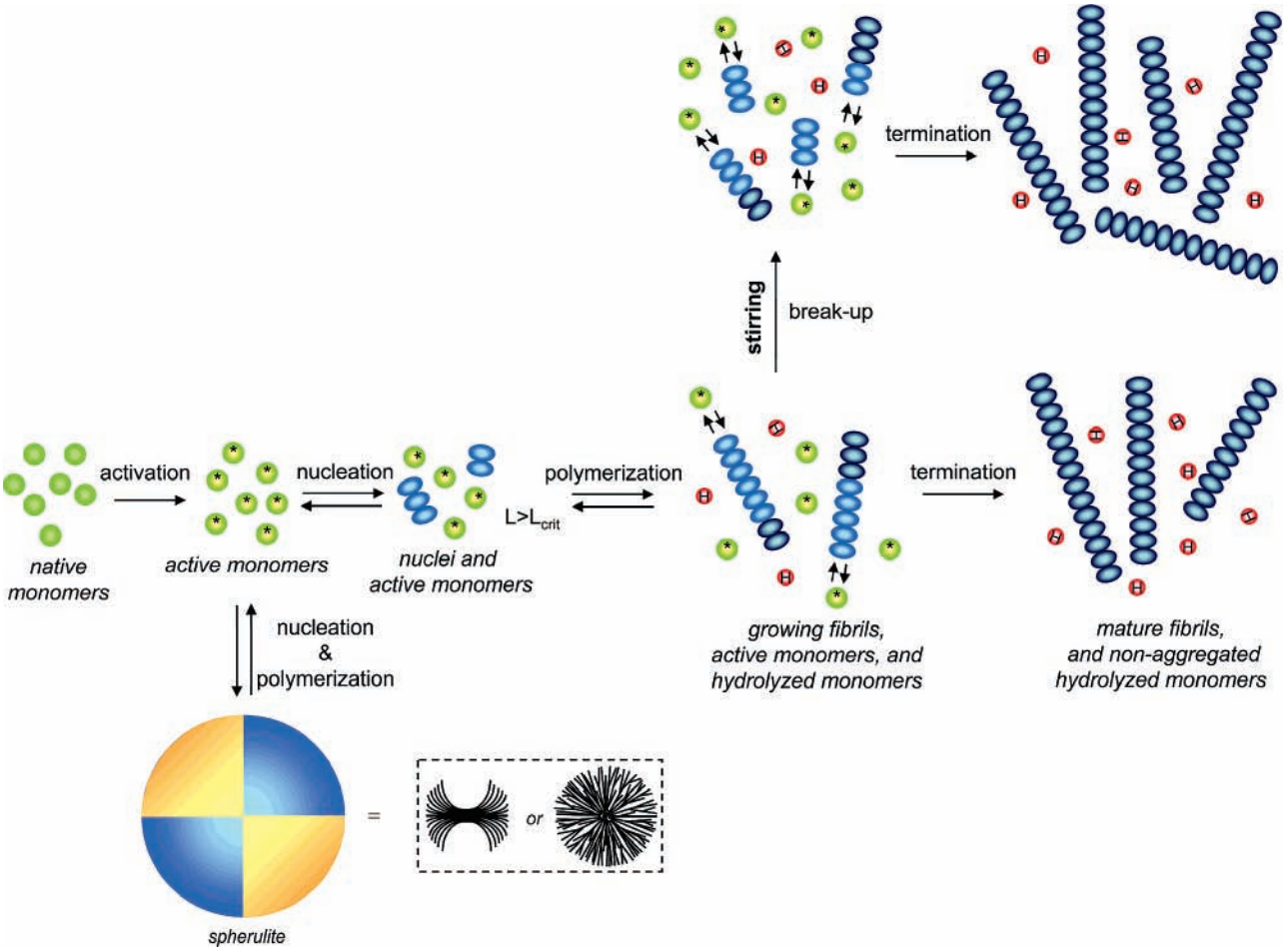

Figure 10. Schematic model for fibril formation at rest or while stirring during heating. Green circles represent protein monomers; activated protein monomers are indicated with an asterisk; reversibly aggregated monomers are represented by connected bright blue ovals; irreversibly connected monomers are represented by connected deep blue ovals; red circles with "H" indicate hydrolyzed monomers. The circle divided in quadrants represents a spherulite as observed with polarized light combined with a red compensator filter. (Note that structures are not drawn to scale.)

Nucleation is the rate-limiting step for fibril growth. Once the nuclei for fibrils in solution have a size exceeding a certain critical value, L_{crit}, polymerization can occur (*54*−*57*). Fibrils grow by addition of monomers, possibly on both ends. Akkermans et al. (*58*) proposed a simple scaling analysis that explains the accelerating effect of shear flow (the sum of rotation and elongation) on fibril growth. Initially the fibril length increases as $L \sim t$ (*58*). When L increases, fibrils start to overlap and the sample will be in a semidilute regime where L increases as $L \sim t^{1/3}$. The fibril growth slows down as L increases until there is an equilibrium between the addition of monomers to the fibril and the removal of monomers. Then L will become constant. The combination of a slow nucleation and fast fibril growth leads to a time dependence of the size distribution as shown in **Figure 6**; in time new fibrils are formed but the peak length does not change significantly. This explains the stop of the growth of a single fibril. When monomers are incorporated in the fibrils, initially they bind reversible. After some time, this bond becomes irreversible, likely due to formation of intermolecular β-sheets (*6*, *52*). When monomers in the fibrils are reversibly bound, we call them immature fibrils. They are still susceptible to breakup in shear flow. Breakup occurs due to the elongational component of shear flow (*58*). When they are mature (β-sheets have formed between monomers in the fibril), they do not breakup as easily anymore. Both Arnaudov et al. (*4*) and Akkermans et al. (*3*) showed with light scattering experiments that β-lg fibrils formed after short heating times at pH 2 are reversible. They do disassemble upon cooling. After longer heating times, the fibrils no longer disassemble upon cooling (*3*, *4*). Mature WPI fibrils do not break up, even after shearing at a rate of 600 s^{-1}, as reported by Akkermans et al (*58*).

Above we have explained why a single fibril stops growing. Here we will explain why the overall reaction terminates. Nonassembled monomers are inactivated due to hydrolysis after prolonged heating (*27*). The fibrils will no longer have active ends due to irreversible aggregation (formation of intermolecular β-sheets) of the monomers or hydrolysis of the fibril ends, thus terminating the reaction. In flow, immature fibrils may be broken up, increasing the number of active fibrils. Flow may also increase the number of encounters between the particles, leading to fast growth of the nuclei and the growing fibrils. As a result, more fibrils are formed when samples are stirred. Seeding only affects the number of fibrils in the initial sample. Prior to heating, preformed fibrils and nonaggregated monomers are present in the sample. These fibrils and monomers are not active anymore and will therefore not contribute to the assembly process. It is possible that other types of seeds (e.g., seeds prepared using shorter heating times) would show an additional effect on fibril formation. After shorter heating times of the seeds, the fibrils and nonassembled monomers are not yet inactivated, and are therefore susceptible to assembly.

We propose that there are two processes that contribute to the termination of fibril formation. The one is lack of active

monomers due to hydrolysis of nonassembled monomers upon prolonged heating. The other is the inactivation of fibril growth ends, possibly due to formation of intermolecular β-sheets or hydrolysis of the fibril ends. Prolonged heating for more than 10 h may induce hydrolysis of mature fibrils. This might be an explanation for the slight decrease in the amount of fibrils for heating times exceeding 10 h, as observed in conversion experiments (**Figure 2**), birefringence measurements (**Figure 3A**), and viscosity measurements.

CONCLUSION

From the present study on the effect of stirring and seeding on the formation of WPI fibrils, we can conclude that stirring during heating is dominant. Samples that were heated while stirring showed a much higher conversion, birefringence, and apparent viscosity than samples that were heated at rest. The length of the fibrils was not significantly different, indicating that more fibrils of a similar length are formed when WPI is stirred during heating at pH 2 and 80 °C. Addition of seeds did not show an additional effect compared to samples that were stirred. The seeds were most likely not active and therefore did not contribute to the fibril formation. Possibly use of other types of seeds (e.g., prepared with shorter heating times) would show an additional effect on the fibril formation next to the effect of stirring during heating. We propose a model for fibril formation, including an activation and nucleation step, a growth step, and a termination step. The activation and nucleation steps are relatively slow and therefore are the rate determining steps. Fibril growth is relatively fast but terminates after prolonged heating. Two processes that possibly induce termination of fibril formation are hydrolysis of nonassembled monomers and inactivation of the growth end of the fibrils. Stirring likely breaks up immature fibrils, thus producing more active fibrils. Stirring also seems to accelerate the kinetics of fibril formation, resulting in an increase of the number of fibrils formed.

ACKNOWLEDGMENT

We gratefully acknowledge Ardy Nijboer for her contribution to the seeding experiments.

LITERATURE CITED

(1) Dobson, C. M. *Semin. Cell Dev. Biol.* **2004**, *15*, 3−16.
(2) Uversky, V. N.; Fink, A. L. *Biochim. Biophys. Acta* **2004**, *1698*, 131−153.
(3) Akkermans, C.; Venema, P.; Rogers, S. S.; van der Goot, A. J.; Boom, R. M.; van der Linden, E. *Food Biophys.* **2006**, *1*, 1557−1858.
(4) Arnaudov, L. N.; de Vries, R.; Ippel, H.; van Mierlo, C. P. M. *Biomacromolecules* **2003**, *4*, 1614−1622.
(5) Aymard, P.; Nicolai, T.; Durand, D.; Clark, A. *Macromolecules* **1999**, *32*, 2542−2552.
(6) Bromley, E. H. C.; Krebs, M. R. H.; Donald, A. M. *Faraday Discuss.* **2004**, *128*, 13−27.
(7) Goers, J.; Permyakov, S. E.; Permyakov, E. A.; Uversky, V. N.; Fink, A. L. *Biochemistry* **2002**, *41*, 12546−12551.
(8) Gosal, W. S.; Clark, A. H.; Pudney, P. D. A.; Ross-Murphy, S. B. *Langmuir* **2002**, *18*, 7174−7181.
(9) Ikeda, S.; Morris, V. J. *Biomacromolecules* **2002**, *3*, 382−389.
(10) Rogers, S. S.; Venema, P.; Sagis, L. M. C.; van der Linden, E.; Donald, A. M. *Macromolecules* **2005**, *38*, 2948−2958.
(11) Veerman, C.; Baptist, H.; Sagis, L. M. C.; van der Linden, E. *J. Agric. Food Chem.* **2003**, *51*, 3880−3885.
(12) Veerman, C.; Sagis, L. M. C.; Heck, J.; van der Linden, E. *Int. J. Biol. Macromol.* **2003**, *31*, 139−146.
(13) Hermansson, A.-M. *J. Agric. Food Chem.* **1985**, *36*, 822−832.
(14) Arnaudov, L. N.; de Vries, R. *Biophys. J.* **2005**, *88*, 515−526.
(15) Krebs, M. R. H.; Wilkins, D. K.; Chung, E. W.; Pitkeathly, M. C.; Chamberlain, A. K.; Zurdo, J.; Robinson, C. V.; Dobson, C. M. *J. Mol. Biol.* **2000**, *300*, 541−549.
(16) Sagis, L. M. C.; Veerman, C.; van der Linden, E. *Langmuir* **2004**, *20*, 924−927.
(17) Veerman, C.; de Schiffart, G.; Sagis, L. M. C.; van der Linden, E. *Int. J. Biol. Macromol.* **2003**, *33*, 121−127.
(18) Weijers, M.; Sagis, L. M. C.; Veerman, C.; Sperber, B.; van der Linden, E. *Food Hydrocolloids* **2002**, *16*, 269−276.
(19) Weijers, M.; van de Velde, F.; Stijnman, A.; van de Pijpekamp, A. M.; Visschers, R. W. *Food Hydrocolloids* **2006**, *20*, 146−159.
(20) Bolder, S. G.; Hendrickx, H.; Sagis, L. M. C.; van der Linden, E. *J. Agric. Food Chem.* **2006**, *54*, 4229−4234.
(21) Gosal, W. S.; Clark, A. H.; Ross-Murphy, S. B. *Biomacromolecules* **2004**, *5*, 2408−2419.
(22) Hamada, D.; Dobson, C. M. *Protein Sci.* **2002**, *11*, 2417−2426.
(23) Kavanagh, G. M.; Clark, A. H.; Ross-Murphy, S. B. *Int. J. Biol. Macromol.* **2000**, *28*, 41−50.
(24) Rogers, S. S. Some Physical Properties of Amyloid Fibrils, in Biological and Soft Systems; Cavendish Laboratory, Cambridge University: Cambridge, UK, 2006; pp 178.
(25) Sagis, L. M. C.; Veerman, C.; Ganzevles, R.; Ramaekers, M.; Bolder, S. G.; van der Linden, E. *Food Hydrocolloids* **2002**, *16*, 207−213.
(26) Veerman, C.; Ruis, H.; Sagis, L. M. C.; van der Linden, E. *Biomacromolecules* **2002**, *3*, 869−873.
(27) Bolder, S. G.; Vasbinder, A. J.; Sagis, L. M. C.; van der Linden, E. *Int. Dairy J.* **2007**, *17*, 846−853.
(28) Nielsen, L.; Khurana, R.; Coats, A.; Frokjaer, S.; Brange, J.; Vyas, S.; Uversky, V. N.; Fink, A. L. *Biochemistry* **2001**, *40*, 6036−6046.
(29) Stathopulos, P. B.; Scholz, G. A.; Hwang, Y.-M.; Rumfeldt, J. A. O.; Lepock, J. R.; Meiering, E. M. *Protein Sci.* **2004**, *13*, 3017−3027.
(30) Hill, E. K.; Krebs, B.; Goodall, D. G.; Howlett, G. J.; Dunstan, D. E. *Biomacromolecules* **2006**, *7*, 10−13.
(31) Bolder, S. G.; Hendrickx, H.; Sagis, L. M. C.; van der Linden, E. *Appl. Rheol.* **2006**, *16*, 258−264.
(32) Fuller, G. G. *Annu. Rev. Fluid Mech.* **1990**, *22*, 387−417.
(33) Klein, C.; Venema, P.; Sagis, L. M. C.; van Dusschoten, D.; Wilhelm, M.; Spiess, H. W.; van der Linden, E.; Rogers, S. S.; Donald, A. M. *Appl. Rheol.* **2007**, *17*, 45210.
(34) Doi, E.; Edwards, P. J. B. *J. Chem. Soc., Faraday Trans. 2* **1978**, *74*, 918−932.
(35) Marrucci, G.; Grizzuti, N. *J. Polym. Sci., Polym. Lett. Ed.* **1983**, *21*, 83−86.
(36) Marrucci, G.; Grizzuti, N. *J. Non-Newtonian Fluid Mech.* **1984**, *14*, 103−119.
(37) Schokker, E. P.; Singh, H.; Pinder, D. N.; Creamer, L. K. *Int. Dairy J.* **2000**, *10*, 233−240.
(38) Bolder, S. G.; Sagis, L. M. C.; Venema, P.; van der Linden, E. *Langmuir* **2007**, *23*, 4144−4147.
(39) Cato, A. D.; Edie, D. D.; Harrison, G. M. *J. Rheol.* **2005**, *49*, 161−174.
(40) Matheson, R. R. *Macromolecules* **1980**, *13*, 643−648.
(41) Fogolari, F.; Ragona, L.; Zetta, L.; Romagnoli, S.; de Kruif, K. G.; Molinari, H. *FEBS Lett.* **1998**, *436*, 149−154.
(42) Nilsson, M. R.; Dobson, C. M. *Protein Sci.* **2003**, *12*, 2637−2641.
(43) Hamodrakas, S. J.; Hoenger, A.; Iconomidou, V. A. *J. Struct. Biol.* **2004**, *145*, 226−235.
(44) Krebs, M. R. H.; Bromley, E. H. C.; Rogers, S. S.; Donald, A. M. *Biophys. J.* **2005**, *88*, 2013−2021.
(45) Krebs, M. R. H.; MacPhee, C. E.; Miller, A. F.; Dunlop, I. E.; Dobson, C. M.; Donald, A. M. *Proc. Natl. Acad. Sci. U.S.A.* **2004**, *101*, 14420−14424.

(46) Rogers, S. S.; Krebs, M. R. H.; Bromley, E. H. C.; van der Linden, E.; Donald, A. M. *Biophys. J.* **2006**, *90*, 1043−1054.
(47) Bassett, D. C. *J. Macromol. Sci., Part B: Phys.* **2003**, *42*, 227−256.
(48) Broide, M. L.; Berland, C. R.; Pande, J.; Ogun, O. O.; Benedek, G. B. *Proc. Natl. Acad. Sci. U.S.A.* **1991**, *88*, 5660−5664.
(49) Chow, P. S.; Zhang, J.; Liu, X. Y.; Tan, R. B. H. *Int. J. Mod. Phys. B* **2002**, *16*, 354−358.
(50) Muschol, M.; Rosenberger, F. *J. Chem. Phys.* **1997**, *107*, 1953−1962.
(51) Rogers, S. S.; Venema, P.; van der Ploeg, J. P. M.; van der Linden, E.; Sagis, L. M. C.; Donald, A. M. *Biopolymers* **2006**, *82*, 241−252.
(52) Krebs, M. R. H.; Bromley, E. H. C.; Donald, A. M. *J. Struct. Biol.* **2005**, *149*, 30−37.
(53) Lefevre, T.; Subirade, M. *Biopolymers* **2000**, *54*, 578−586.
(54) Flyvbjerg, H.; Jobs, E.; Leibler, S. *Proc. Natl. Acad. Sci. U.S.A.* **1996**, *93*, 5975−5978.
(55) Kelly, J. W. *Nat. Struct. Biol.* **2000**, *7*, 824−826.
(56) Lomakin, A.; Chung, D. S.; Benedek, G. B.; Kirschner, D. A.; Teplow, D. B. *Proc. Natl. Acad. Sci. U.S.A.* **1996**, *93*, 1125−1129.
(57) Lomakin, A.; Teplow, D. B.; Kirschner, D. A.; Benedek, G. D. *Proc. Natl. Acad. Sci. U.S.A.* **1997**, *99*, 7942−7947.
(58) Akkermans, C.; van der Goot, A. J.; Venema, P.; van der Linden, E.; Boom, R. M. submitted for publication.

Received for review November 20, 2006. Revised manuscript received April 18, 2007. Accepted May 4, 2007.

JF063351R